



## Removal of copper(II) and nickel(II) ions from aqueous solution using non-living lichen *Ramalina fraxinea* biomass: investigation of kinetics and sorption isotherms

Mehmet Candan<sup>a,\*</sup>, Funda Tay<sup>b</sup>, Ilker Avan<sup>c</sup>, Turgay Tay<sup>c</sup>

<sup>a</sup>Department of Biology, Faculty of Science, Anadolu University, Eskişehir 26470, Turkey, Tel. +90 222 335 0580–4720; Fax: +90 222 320 4910; email: mecandan@anadolu.edu.tr

<sup>b</sup>Department of Chemistry, Faculty of Arts & Sciences, Eskişehir Osmangazi University, Eskişehir 26480, Turkey, email: ftay@ogu.edu.tr

<sup>c</sup>Department of Chemistry, Faculty of Science, Anadolu University, Eskişehir 26470, Turkey, emails: iavan@anadolu.edu.tr (I. Avan), turgaytay@gmail.com (T. Tay)

Received 23 September 2016; Accepted 23 March 2017

### ABSTRACT

Studies in the field of heavy metal ion removal from industrial wastewater using biomass are increasing in number due to highly efficient and cost-effective applications. In this study, we report the use of non-living lichen, *Ramalina fraxinea*, as a biosorbent for the removal of Cu(II) and Ni(II) ions from aqueous solution. The biosorption of Cu(II) and Ni(II) ions from aqueous solution by *R. fraxinea* biomass is investigated in a batch system for parameters such as pH, contact time, and initial concentrations of metal ions. The kinetic data of the biosorption process is evaluated with pseudo-first-order, pseudo-second-order and intraparticle diffusion kinetic models. The experimental data shows greater accordance with the pseudo-second-order model for the tested ions. The equilibrium data of Cu(II) and Ni(II) ions biosorption fitted onto both the Langmuir and Freundlich adsorption models. The highest sorption capacities of Cu(II) and Ni(II) ions by the *R. fraxinea* biomass are found to be 43.48 and 9.71 mg/g, respectively. The biosorption studies indicate that *R. fraxinea* biomass is a moderate biosorbent for the removal of Cu(II) and Ni(II) ions from aqueous solutions compared with other biosorbents.

**Keywords:** Biosorption; Copper; Nickel; Isotherms; Kinetics; Lichen

### 1. Introduction

Heavy metals can cause irreversible environmental defects due to intrusion into biological processes in living organisms. As heavy metals are non-biodegradable substances, they cannot be dismissed by nature and, thus, show accumulation in living organisms once they enter into the food chain [1,2]. Heavy metals such as antimony (Sb), arsenic (As), chromium (Cr), cadmium (Cd), lead (Pb) and mercury (Hg) are listed as toxic even in small quantities by the World Health Organization (WHO) [3]. Others including copper (Cu), nickel (Ni) and selenium (Se) are essential

micronutrients for bioprocesses and should be included in a daily diet [3]. However, adverse effects may result from excessive use or prolonged exposure to these heavy metals [4,5]. The transfer of heavy metals to humans brings serious health disorders in neural, renal and respiratory systems by inhibiting the functions of biomaterials (proteins, enzymes and suchlike) and may cause cancer and multiple organ damage by accumulative poisoning [3–6]. The WHO emphasizes the maximum permissible limit for certain heavy metals in drinking water as follows: Sb (0.02 mg/L); As (0.01 mg/L); Cr (0.05 mg/L); Cd (0.003 mg/L); Pb (0.01 mg/L); Hg (0.006 mg/L); Se (0.04 mg/L); Cu (2.0 mg/L) and Ni (0.07 mg/L) [3]. Industrial processes including mining, metal smelt-plating, manufacture of chemicals, electronic devices and batteries

\* Corresponding author.

are the main sources of heavy metal waste [6]. Inadequate disposal of such waste effluent also contributes to an increase in heavy metal distribution and abundance in nature. Therefore, it is highly important to eliminate heavy metals from industrial waste effluent to keep natural sources clean. Water remediation systems that are used alone or in combination with conventional methods, such as precipitation, adsorption, flocculation, membrane filtration, coagulation, reverse osmosis, ion-exchange resins, electrodialysis and electrodeposition, have limited use because of high operational costs, high reagent-energy demands, generation of secondary waste and insufficient effectiveness at low metal concentrations (1–100 mg/L) [6–10]. Adsorption is a highly appreciable technique due to its high efficacy even at low metal ion concentrations [10]. A wide variety of sorption media, including synthetic–natural polymers, activated carbon, zeolites and biomaterials, are used as adsorption material with various sorption capacity and cost [6,11–15]. Biosorption is the use of dead or live biomaterials as adsorbent, such as agricultural waste-based materials (wheat straw, fruit peel, husk, bark, leaves and suchlike), animal-based materials (bones, sheep-cow hoof and suchlike), bacteria or its components, fungi, algae and moss [6,10,16–37]. Many of these biosorbents are available in high quantities with low cost or which are free of charge that reduces operational costs. Recently, lichens have also been employed as biosorbent for the removal of heavy metal ions from aqueous solutions [38,39]. Lichens are composed of mutually living organisms, including a fungus and a green algae or a cyanobacterium [40]. Lichens have a rich composition of polymeric and non-polymeric compounds featuring a variety of metal binding sites, such as cellulose, hemicellulose, chitin, aromatic, phenolic, carboxylic acid derivatives and others [40,41]. Lichens are considered as bioindicators of environmental pollution because of their sensitivity to a variety of pollutants [40]. Living lichens can accumulate metal ions by ion exchange, extracellular adsorption and particle trapping [42]. Their natural abundance and cost-effective value make lichens suitable biosorbent for the removal of metal ions from aqueous solutions. Accordingly, non-living lichens have recently been employed for the exclusion of heavy metal from aqueous solutions [38,43–46].

In this study, we report the use of a common non-living fruticose lichen, *Ramalina fraxinea*, which grows on the nutrient-rich bark of broad-leaved trees (Fig. 1), as a biosorbent for the removal of Cu(II) and Ni(II) ions from aqueous solution. The effects of various parameters, such as pH, contact time and initial concentrations of metal ions on the biosorption capacity, are examined. The kinetic data of the biosorption process are evaluated using pseudo-first-order kinetic model, pseudo-second-order kinetic model and the intraparticle diffusion model. Langmuir and Freundlich isotherm equations are used to determine the capacity and mechanism of the biosorption process of tested metal ions onto the *R. fraxinea* biomass.

## 2. Experiments

### 2.1. Preparation of *R. fraxinea* biomass

The lichen, *R. fraxinea*, was collected from the TEMA Forest, Bozdağ, Eskişehir Province, Turkey, at an altitude of

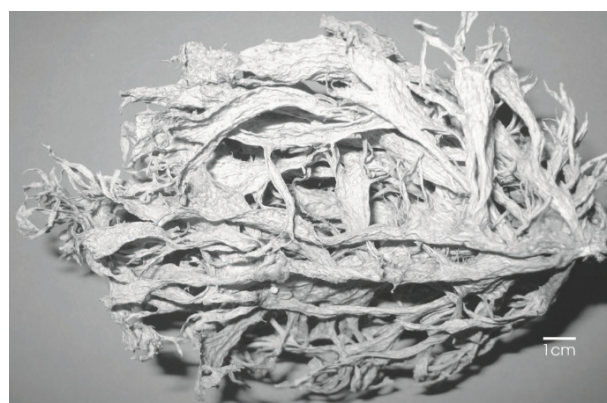


Fig. 1. Thallus of *R. fraxinea*.

1,100 m. *R. fraxinea* samples were stored at the Herbarium of Department of Biology (ANES) at Anadolu University. The samples were washed several times with distilled water to remove adhered dirt and dried at 50°C for 24 h. The dried samples were ground and sieved into the following sizes; 0–75, 75–125, 125–250 and 250–500  $\mu\text{m}$ . Otherwise specified, the *R. fraxinea* biomass of 75–125  $\mu\text{m}$  size was employed in all of the biosorption experiments.

### 2.2. Biosorption experiments

The biosorption of Cu(II) and Ni(II) ions onto the *R. fraxinea* biomass from the aqueous solutions was investigated in batch experiments using 100 mg of *R. fraxinea* biomass in 25 mL solution in Erlenmeyer flasks, in a water bath at 25°C. The adsorption media was stirred with continuous agitation of 200 rpm. 250 ppm Cu(II) and 200 ppm Ni(II) ions solutions were used for the investigation of pH and contact time on the biosorption. The effect of pH on the biosorption capacity of the biomass for metal ions was investigated in a pH range of 1.0–6.0 at 25°C. The pH values of the sorption medium were adjusted using a pH meter to the desired value by adding 0.1 M HCl or 0.1 M NaOH at the beginning of experiments and were not further controlled. The pH effect was measured after treating with biosorbent for 240 min, which was sufficient time to reach sorption equilibrium. Experimental control tests were conducted in the absence of the biosorbent in order to determine the Cu(II) and Ni(II) removal by chemical precipitation and sorption onto the vessel walls. The effect of contact time on biosorption was examined using the same amount of *R. fraxinea* biomass (100 mg) in 50 mL metal ion solutions (50–500 mg/L) in a time range of 0–180 min at pH 5.0 for Cu(II) and at a pH of 6.0 for Ni(II) ions. The effect of the initial metal ions concentration on the biosorption was investigated using single metal ion solutions at different concentrations, ranging from 50 to 500 mg/L. After the biosorption media reached equilibrium for both ions, the mixtures were centrifuged at 4,500 rpm for 5 min, and the concentrations of Cu(II) or Ni(II) ions in aqueous phase were analyzed using an atomic absorption spectrophotometer (AAS) with an air-acetylene flame (Perkin Elmer AAnalyst 800 Model). The AAS instrument responses were periodically tested using standard Cu(II) or Ni(II) ion solutions. The amounts of adsorbed metal ions ( $q_t$ ) per gram of

biomass at equilibrium were calculated by subtracting the final metal ion concentrations from the initial metal concentrations in the solution, as stated in Eq. (1):

$$q_e = \frac{(C_0 - C_e)V}{m} \quad (1)$$

where  $q_e$  (mg/g) is the amount of adsorbed metal ion onto the biomass;  $C_0$  (mg/L) is the initial metal concentration in the solution;  $C_e$  (mg/L) is the final metal ion concentration at equilibrium;  $V$  (L) is the volume of the solution; and  $m$  (g) is the amount of biomass employed in the adsorption process.

Adsorption isotherm experiments were performed after ensuring optimum adsorption conditions (240 min contact time at pH 5.0 for Cu(II) and at pH 6.0 for Ni(II) ions) starting with different metal ion concentrations (ranging between 50 and 500 ppm) at a constant temperature (25°C).

Adsorption kinetics were evaluated by analyzing instant concentration of Cu(II) and Ni(II) ions in aqueous solution within certain time intervals up to 180 min, with the concentrations of metal ions being measured as in the equilibrium tests. Kinetic studies were performed using 100 mg adsorbent in 50 mL of 250 ppm Cu(II) or 200 ppm Ni(II) ion solutions at a constant temperature of 25°C.

### 2.3. Analytical determination

The pH values were measured using an Orion 420A pH meter. The amount of free metal ions in the solutions was determined using a Perkin-Elmer AAnalyst 800 Model AAS equipped with an air-acetylene flame. The working currents/wavelengths for the metal ions Cu(II) and Ni(II) were 4.0 mA/324.8 nm and 4.0 mA/232.0 nm, respectively. Calibration solutions for the AAS instrument were prepared from stock solutions (for Ni(II) ions,  $1,000 \pm 2$  mg Ni(NO<sub>3</sub>)<sub>2</sub> and were dissolved in 1,000 mL water; and for Cu(II) ions,  $1,000 \pm 2$  mg Cu metal was dissolved in 10 mL concentrated HNO<sub>3</sub> and diluted to 1,000 mL with water). The instrument responses were periodically checked by standard metal solutions. Experiments were conducted in triplicate and averaged. The scanning electron microscope (SEM) images of the biomass were obtained by a Carl Zeiss ultra plus field-emission SEM. The specific surface areas of the biomass was measured

by the N<sub>2</sub> adsorption technique (at 77 K), using a surface analyzer (NOVA 2200e, Quantachrome Instruments, USA). The isoelectric point (IEP) of the *R. fraxinea* biomass was determined by using a Malvern Zetasizer Nano ZS potentiometer equipped with an MPT-2 multipurpose autotitrator. The pH solution was adjusted by adding either hydrochloric acid (0.025 and 0.5 M) or sodium hydroxide (0.15 M) solution during the zeta potential measurements. The FTIR spectra were recorded on a PerkinElmer 100 FT-IR spectrometer.

### 2.4. Characterization

An SEM analysis was carried out to determine the surface morphology of the *R. fraxinea* biomass. SEM images of the *R. fraxinea* biomass (Fig. 2) show rough microtubular structures within an irregular surface. The cryogenic gas sorption (based on Brunauer–Emmett–Teller (BET) theory) of *R. fraxinea* biomass is of mean at 12.91 m<sup>2</sup>/g total pore volume and is almost equal to mesopore volume (Table 1). The zeta potential of the *R. fraxinea* biomass was investigated in our previously published study depending on pH [43]. The isoelectric point (IEP) was determined as 6.72 in the pH scale. Beyond this pH, the biomass surface was negatively charged.

The functional groups that are present in the surface of *R. fraxinea* biomass are characterized by FTIR spectroscopic studies. Fig. 3 shows the FTIR spectra of *R. fraxinea* biomass and those ion-loaded. On the FTIR spectra of natural *R. fraxinea* biomass, a strong band around 3,398 cm<sup>-1</sup> designates the presence of hydroxyl (–OH) or amido (–NH–) groups, and a peak at 2,928 cm<sup>-1</sup> represents the stretching frequency of C–H groups. The weak signal at 1,721 cm<sup>-1</sup> might show the stretching vibration of C=O of ester and carboxylic acid functionality. The strong peak at 1,653 cm<sup>-1</sup> shows amide C=O stretching, while the peak at 1,541 cm<sup>-1</sup> shows amide N–H bending and the band at 1,375 cm<sup>-1</sup> corresponds to the symmetrical deformation of amides, which are the characteristic signals for chitin structure [47,48]. The band at 1,039 cm<sup>-1</sup> shows C–O stretching of alcohols and carboxylic acids. When the *R. fraxinea* biomass adsorbs metal ions, the strong band around 3,398 cm<sup>-1</sup> due to hydroxyl or amido groups became broader, and the stretching vibrations of carbonyl groups (C=O) were shifted to 1,724 and 1,657 cm<sup>-1</sup>. The FTIR results suggest that the hydroxyl and carbonyl groups of acids and amides



Fig. 2. SEM images of the *R. fraxinea* biomass.

present on the surface of the *R. fraxinea* biomass participate in the complex formation with metal ions.

### 3. Results and discussion

#### 3.1. Effect of pH on the biosorption of Cu(II) and Ni(II) ions

Biosorption of metal ions onto biomass is highly pH dependent since it affects the solubility of metals and the ionization state of various functional groups (carboxylate, phosphate and amino groups) on the biosorbent surface. The aforementioned functional groups usually built metal–organic complexes with metal cations through electrostatic interactions. A rise in pH increases the number of negatively charged functional groups that form better binding sites for metal cations, whereas after certain pH values, the metal ion concentration decreases due to the precipitation of metal ions as hydroxides in a basic condition. Therefore, the metal adsorption capacity of a biomass is determined by the cooperation of these two pH dependent parameters. Sheng et al. previously showed the existence of a percentage of various metal ions (Pb(II), Cu(II), Cd(II), Ni(II) and Zn(II)) in aqueous solutions as a function of pH [49]. It was calculated that the Cu(II) ion was the dominant species below pH 5.2 and Ni(II) ion was the dominant species below pH 7.5 in aqueous solutions [49]. Herein, biosorption experiments were carried out under acidic conditions ranging from of 1.0 to 5.0 for Cu(II) and from 1.0 to 6.0 for Ni(II), to prevent metal hydroxide precipitations. Fig. 4 shows Cu(II) and Ni(II) uptake onto the *R. fraxinea* biomass as a function of pH. It was observed that the biosorption capacities were increased by increasing the pH value of the solution. The highest biosorption capacities were achieved for Cu(II) at pH 5.0 and for Ni(II) ions at pH 6.0, which is 23.2 mg/g for Cu(II) and 8.35 mg/g for Ni(II). As expected, the *R. fraxinea* biomass surface became more negatively charged, and the metal ion uptakes improved along with an increase in pH. Experimental control tests also indicated that the metal ion uptakes were purely based on biosorption.

Table 1  
Surface and pore characteristics of the *R. fraxinea* biomass

<i>R. fraxinea</i> biomass	
BET surface area (m <sup>2</sup> /g)	12.91
Mesopore surface area (m <sup>2</sup> /g)	12.91
Average pore diameter (Å)	19.9
Mesopore volume (cm <sup>3</sup> /g)	0.0129

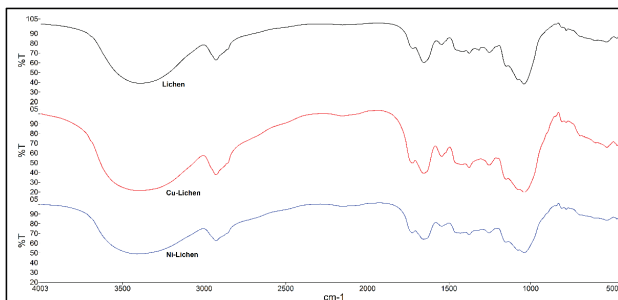


Fig. 3. FTIR spectra of *R. fraxinea* biomass and those ion-loaded.

#### 3.2. Effect of contact time on biosorption

The effect of contact time on the biosorption of metal ions (100 mg/L) on *R. fraxinea* biomass was investigated within the time range of 0–180 min at 25°C. Fig. 5 shows the time course of Cu(II) and Ni(II) ions adsorption on the *R. fraxinea* biomass for Cu(II) at pH 5 and for Ni(II) ions at pH 6. As can be seen in Fig. 5, the Cu(II) ion uptake showed a rapid increase in the first 40 min of contact time, and after this, the Cu(II) adsorption appeared to reach equilibrium. After 50 min, the Cu(II) ion uptake again started a gradually increase. Ni(II) ion uptake showed a rapid increase in the first 10 min, and then it showed a slow increase between 20 and 30 min. It received a gradual increment up to 90 min, and beyond this time it reached equilibrium and did not show any significant Ni(II) uptake.

#### 3.3. Effect of initial Cu(II) and Ni(II) ions concentration on the biosorption

The effect of the initial Cu(II) and Ni(II) ions concentration ( $C_0$ ) on the biosorption capacity of *R. fraxinea* biomass was studied using single ion concentrations (50–500 mg/L) at optimum conditions (pH 5 for Cu(II) and pH 6 for Ni(II) ions

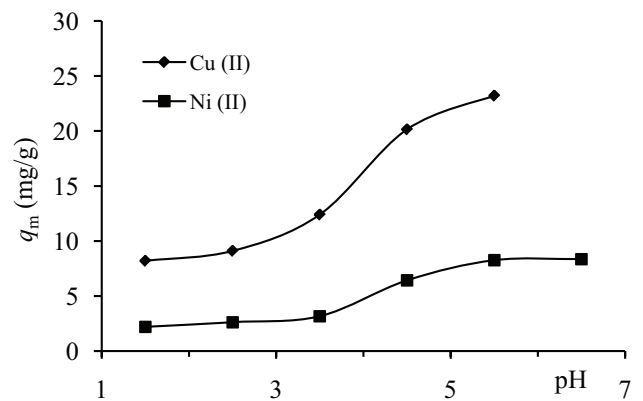


Fig. 4. Effect of pH on the biosorption of Cu(II) and Ni(II) ions by the *R. fraxinea* biomass.

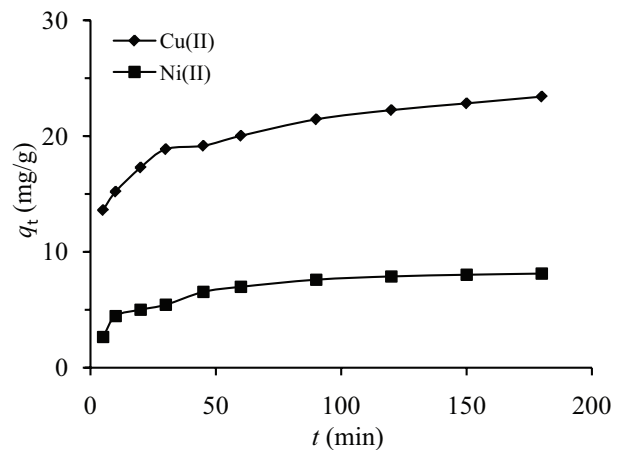


Fig. 5. Effect of contact time for Cu(II) and Ni(II) biosorption by the *R. fraxinea* biomass.

with 240 min contact time). It is well known that initial concentration is a main driving force for overcoming mass transfer resistance between aqueous and solid phases. Herein, the Cu(II) and Ni(II) uptake first increased with increasing initial metal ion concentrations because of a greater probability for metal ions to bind the active adsorption sites on the biosorbent surface (Fig. 6). The Ni(II) adsorption capacity became constant after  $C_0$  of 300 mg/L, since the sorption sites on the biosorbent surface became saturated. The Cu(II) uptake showed small increments after 300 mg/L of  $C_0$  due to existing active sites.

### 3.4. Kinetics of the biosorption

Kinetic models are used to understand the sorption mechanism and evaluate the adsorbent performance for metal ion uptake. Various kinetic models, including the pseudo-first-order, pseudo-second-order and intraparticle diffusion, were applied to determine the efficiency and biosorption mechanism of Cu(II) and Ni(II) on the *R. fraxinea* biomass. The kinetic rate equations for first-order (Eq. (2)), second-order (Eq. (3)) and intraparticle diffusion (Eq. (4)) are represented below [50]:

$$\ln(q_1 - q_t) = \ln q_1 - k_1 t \quad (2)$$

$$\frac{t}{q_t} = \frac{1}{k_2 q_2^2} + \frac{1}{q_2} t \quad (3)$$

$$q_t = k_{dif} \sqrt{t} + c \quad (4)$$

where  $q_t$  is the amount of biosorbed metal ions over time (mg/g);  $q_1$  and  $q_2$  are the amounts of biosorbed metal ions at equilibrium for the first- and second-order biosorption, respectively (mg/g);  $k_1$  is the pseudo-first-order rate constant (1/min);  $k_2$  is the second-order adsorption rate constant (g/(mg.min)); and  $k_{dif}$  is intraparticle diffusion rate constant (mg/g h<sup>1/2</sup>) for biosorption, with  $c$  being the intercept.

The relevance of the experimental data to the kinetic models was determined by comparing the correlation coefficients

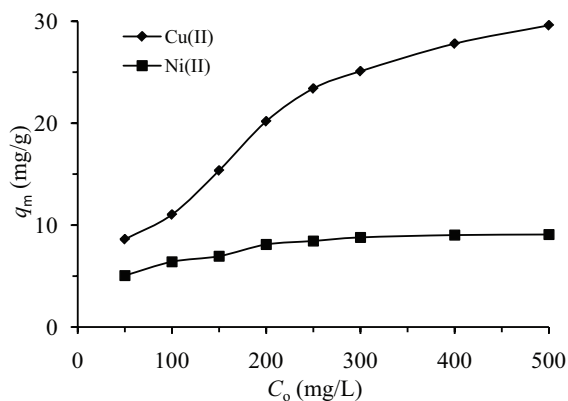


Fig. 6. Effect of the initial ion concentration ( $C_0$ ) on the biosorption of Cu(II) and Ni(II) ions onto the *R. fraxinea* biomass.

( $R^2$ ) of the experiments. (The more applicable model had the relatively higher  $R^2$  value.) To examine the first-order kinetic rate,  $\ln(q_1 - q_t)$  was plotted against  $t$  (Fig. 7). The values of the pseudo-first-order rate constant  $k_1$  were obtained from the slopes of the trend lines. The  $k_1$  values, the correlation coefficients ( $R^2$ ), and theoretical and experimental  $q_1$  values are shown in Table 2. According to the correlation coefficients ( $R^2$ ), the plots do not provide a well-fitted straight line, which indicates that this sorption process is not really applicable for the pseudo-first-order kinetics (Fig. 7). Furthermore, calculated  $q_1$  values are lower than those experimental  $q_1$  values.

The second-order kinetic rate was investigated by plotting of  $t/q_t$  vs.  $t$  (Fig. 8). The plots provided well-fitted straight lines having high correlation coefficients ( $R^2$ ). The values of  $k_2$  and  $q_2$  were calculated from the slope and  $y$ -intercept of the trend line (Table 2). Furthermore, the theoretical values of  $q_2$  obtained from the second-order equation, were fairly close to the experimental values of  $q_{ex}$  (Table 2). These results suggest that the biosorptions of Cu(II) and Ni(II) ions on

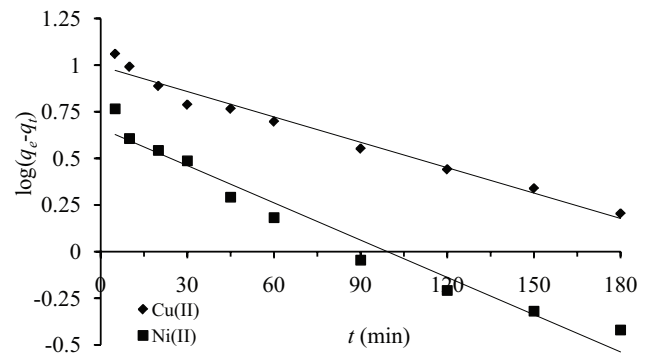


Fig. 7. First-order kinetic plot for Cu(II) and Ni(II) uptake by the *R. fraxinea* biomass.

Table 2  
Kinetic parameters from the pseudo-first-order, pseudo-second-order and intraparticle diffusion models for the adsorption of Cu(II) and Ni(II) ions onto the *R. fraxinea* biomass

	Cu(II)	Ni(II)
$q_{ex}$ (mg/g)	23.4	8.12
Pseudo-first order		
$k_1$ (1/min)	0.0104	0.0154
$q_1$ (mg/g)	9.89	4.59
$R_1^2$	0.974	0.961
Pseudo-second order		
$k_2$ (g/(mg.min))	$5.1 \times 10^{-3}$	$8.35 \times 10^{-3}$
$q_2$ (mg/g)	23.98	8.73
$R_2^2$	0.998	0.999
Intraparticle diffusion		
$k_p$ (mg/(g.min <sup>-1/2</sup> ))	1.158	0.7168
$C$	11.60	1.62
$R_p^2$	0.943	0.938

the *R. fraxinea* biomass could be better described via the pseudo-second-order kinetic model.

To investigate intraparticle diffusion, the amounts of bio-sorbed metal ions over time,  $q_t$ , are plotted against the square root of time ( $t^{1/2}$ ; Fig. 9). A straight line with high correlation coefficients  $R^2$  indicates that intraparticle diffusion might be the rate-limiting step for metal uptakes.  $k_{diff}$  and  $c$  values are obtained from the slope and  $y$ -intercept of these trend lines (Table 2). As can be seen in Fig. 9, none of these trend lines pass through the origin, which implies that intraparticle diffusion is not the only rate-controlling step [51].

### 3.5. Adsorption isotherms

The relationship between the amount of adsorbed substance and its concentration at equilibrium is determined using an adsorption isotherm [24,32,50]. The Langmuir and Freundlich isotherm equations are the most frequently used adsorption isotherm to understand the adsorption mechanism in biosorption studies.

The Langmuir isotherm is only for valid homogenous surfaces on which a single adsorption layer is built [50,52]. The model assumes that the sorbent surface has the uniformity of adsorption sites and the transmigration of adsorbate is not

allowed in the plane of the surface. The linearized Langmuir isotherm is represented by following equation (Eq. (5)):

$$\frac{C_e}{q_e} = \frac{1}{q_m K_L} + \frac{C_e}{q_m} \tag{5}$$

where  $C_e$  (mg/L) and  $q_e$  (mg/g) are defined as the metal ion concentrations at equilibrium and the amount of adsorbed ion onto per gram of adsorbent at any time, respectively.  $K_L$  (L/mg) is the Langmuir isotherm constant related to affinity, and  $q_m$  (mg/g) is the maximum monolayer coverage, which reflects the adsorption capacity.

The Langmuir isotherm model for Cu(II) and Ni(II) ions biosorption onto the *R. fraxinea* biomass was evaluated by plotting graphs between  $C_e/q_e$  vs.  $C_e$  (Fig. 10).  $q_{max}$  and  $K_L$  were computed from the slope and  $y$ -intercept of the trend line, respectively, and are shown in Table 3.

The Freundlich isotherm is used to describe the adsorption mechanism on heterogeneous surfaces that consists of non-uniform adsorption sites of varying affinities and that allows the building of multiple adsorption layers [50,52]. The empirical relationship between the adsorbate concentration and the solute concentration is given by the following equation (Eq. (6)):

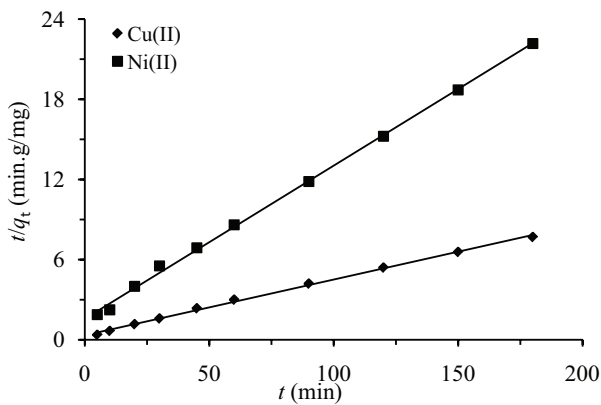


Fig. 8. Second-order kinetic plot for Cu(II) and Ni(II) uptake by the *R. fraxinea* biomass.

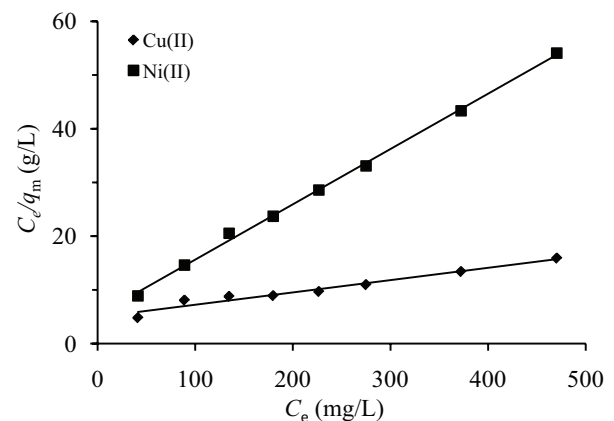


Fig. 10. Langmuir isotherm model for Cu(II) and Ni(II) ions biosorption onto the *R. fraxinea* biomass.

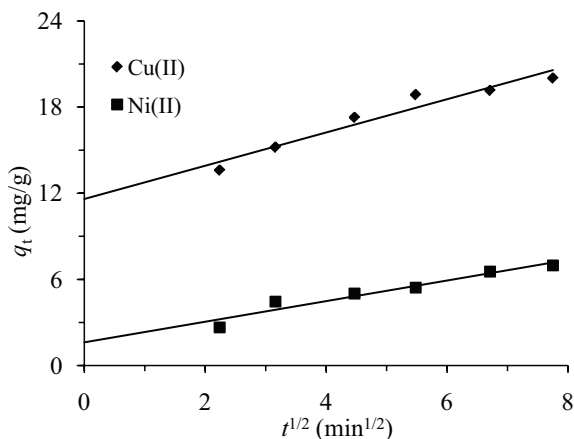


Fig. 9. Intraparticle diffusion model plot for Cu(II) and Ni(II) uptake by the *R. fraxinea* biomass.

Table 3  
Langmuir and Freundlich model equation parameters estimated from the fitting of experimental points of Cu(II) and Ni(II) ions biosorption

	Cu(II)	Ni(II)
Langmuir equation		
$q_{max}$ (mg/g)	43.48	9.71
$K_L$ (L/mg)	0.0047	0.0193
$R^2$	0.960	0.998
Freundlich equation		
$K_F$ (L/mg)	1.02	2.02
$N$	1.79	3.91
$R^2$	0.967	0.956

$$\log q_e = \log K_F + \frac{1}{n} \log C_e \quad (6)$$

where  $C_e$  (mg/L) is the equilibrium concentration of the adsorbate, and  $q_e$  (mg/g) is the amount of substance adsorbed per gram of the adsorbent at equilibrium.  $K_F$  and  $1/n$  are Freundlich constants.  $K_F$  is defined as the adsorption capacity and represents the quantity of adsorbed ions on an adsorbent at equilibrium. The  $1/n$  value indicates the adsorption intensity or surface heterogeneity. Based on the Freundlich isotherm, the  $1/n$  value approaches zero when the surface heterogeneity increases [24,43,50,53]. The Freundlich equilibrium constant was calculated from the plot of  $\log C_e$  vs.  $\log q_m$  in Fig. 11 and is given in Table 3, on the basis of Cu(II) and Ni(II) ions adsorptions onto the *R. fraxinea* biomass.

The relevance of the isotherm equations was evaluated by comparing their correlation coefficients,  $R^2$ . On the basis of Cu(II) biosorption by *R. fraxinea* biomass, experimental data equally fitted on both the Langmuir and Freundlich isotherms, as is reflected with correlation coefficients ( $R^2 = 0.960$  and  $0.967$ , respectively; Table 3). In the case of Ni(II) biosorption, the Langmuir isotherm ( $R^2 = 0.998$ ) showed a better correlation with the experimental data than the Freundlich model ( $R^2 = 0.956$ ). Therefore, the experimental data suggests that single adsorption layers are formed for Ni(II) biosorption. Previously published results for the biosorption of Cu(II) and Ni(II) ions by various biosorbents are given in Table 4. It appears that the *R. fraxinea* biomass moderately removes the tested metal ions compared with other biosorbents.

### 3.6. Adsorption thermodynamics

The determination of thermodynamic parameters is of great importance when assessing whether or not the biosorption process is spontaneous. Experimental data obtained at different temperatures is used to calculate thermodynamic parameters. The changes in free energy ( $\Delta G^\circ$ ), enthalpy ( $\Delta H^\circ$ ) and entropy ( $\Delta S^\circ$ ) of the biosorption processes can be calculated from the distribution constants ( $K_D$ ) using the following equations [63,64]:

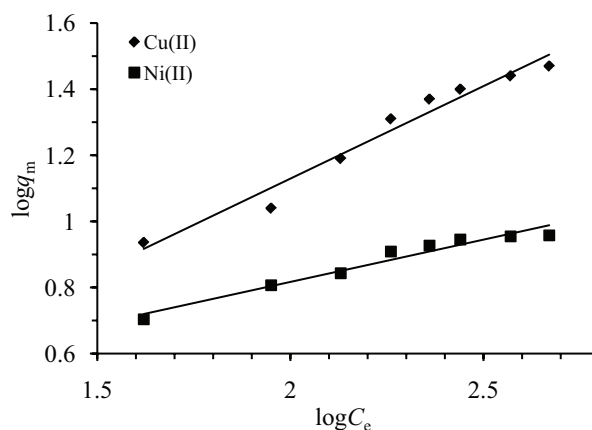


Fig. 11. Freundlich isotherm for Cu(II) and Ni(II) ions biosorption onto the *R. fraxinea* biomass.

Table 4  
Literature survey for the biosorption of Cu(II) and Ni(II) ions onto various biosorbents

Biosorbent material	Cu(II)		Ni(II)		Reference
	Biosorption capacity (mg/g)	pH	Biosorption capacity (mg/g)	pH	
HCl-modified sawdust (oak tree)	3.22	4.0	3.29	8.0	[54]
Formaldehyde-modified mangrove barks	7.25	5.0	6.95	5.0	[55]
Sawdust (teak wood)	4.94	5.24	8.05	5.16	[56]
Dye-loaded sawdust (teak wood)	8.07	5.24	9.87	5.16	[56]
Groundnut shells	4.46	5.24	3.83	5.16	[56]
Dye-loaded groundnut shells	7.60	5.24	7.49	5.16	[56]
Honeycomb	56.52	5.0	52.71	5.0	[57]
HNO <sub>3</sub> -modified corn silk	96.15	6.0	76.92	6.0	[58]
<i>Parkia biglobosa</i> pulp	–	–	143.1	6.0	[59]
Macroalgae ( <i>Sargassum</i> sp.)	62.8	5.0	35.8	5.5	[49]
Macroalgae ( <i>Padina</i> sp.)	72.4	5.0	37.0	5.5	[49]
Algae ( <i>Codium vermilara</i> )	16.9	5.0	13.2	6.0	[60]
Algae ( <i>Fucus spiralis</i> )	70.9	4.0	50.0	6.0	[60]
Bacteria ( <i>Pseudomonas</i> sp.)	3.62	4.5	129.55	4.5	[61]
Buriti fibers from <i>Mauritia flexuosa</i> (palm tree)	143.11	5.5	103.71	5.5	[62]
Lichen ( <i>Cladonia rangiformis</i> )	7.69	5.0	–	–	[38]
Lichen ( <i>R. fraxinea</i> )	43.5	5.0	9.7	6.0	This study

$$K_D = \frac{C_0 - C_e}{C_e} \quad (7)$$

$$\Delta G^\circ = -RT \ln K_D \quad (8)$$

$$\ln K_D = \frac{\Delta S^\circ}{R} - \frac{\Delta H^\circ}{RT} \quad (9)$$

$$\Delta G^\circ = \Delta H^\circ - T\Delta S^\circ \quad (10)$$

where  $K_D$  is the distribution constant;  $C_0$  (mg/L) is the initial metal concentration in the solution; and  $C_e$  (mg/L) is the final metal ion concentration at equilibrium.  $R$  (8.314 J/(K.mol)) is the universal gas constant.

According to Eq. (9), if  $1/T$  is plotted against  $\ln K_D$ , the slope of the trend line provides  $\Delta H^\circ/R$ , and the  $y$ -axis intercept gives  $\Delta S^\circ/R$  (Fig. 12). The calculated values of  $\Delta G^\circ$ ,  $\Delta H^\circ$  and  $\Delta S^\circ$  of sorption processes are given in Table 5.

Positive values of  $\Delta G^\circ$  indicate that these sorption processes are non-spontaneous and energy demanded, and so stirring of the mixture is required [65]. The positive values of  $\Delta H^\circ$  also confirm these endothermic processes. The positive values of  $\Delta S^\circ$  indicate there is an increase in the irregularity of the metal ions on the liquid/biomass interface.

#### 4. Conclusions

Heavy metal ions, Cu(II) and Ni(II), were successfully removed from the aqueous solution by the non-living lichen (*R. fraxinea*) biomass. Sorption studies indicate that

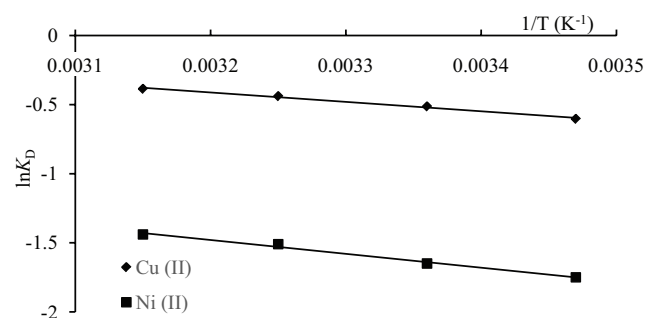


Fig. 12. Plot of  $\ln K_D$  vs.  $1/T$  for estimation of thermodynamic parameters of biosorption.

Table 5  
Thermodynamic parameters for biosorptions of Cu(II) and Ni(II) onto prepared biomass

T (K)	Cu(II)			Ni(II)		
	$\Delta G^\circ$ (kJ/mol)	$\Delta H^\circ$ (kJ/mol)	$\Delta S^\circ$ (J/K.mol)	$\Delta G^\circ$ (kJ/mol)	$\Delta H^\circ$ (kJ/mol)	$\Delta S^\circ$ (J/K.mol)
288.15	1.45	5.65	14.63	4.19	8.33	14.35
298.15	1.27			4.09		
308.15	1.13			3.92		
318.15	1.02			3.79		

the biosorption of Cu(II) and Ni(II) onto *R. fraxinea* biomass were affected by experimental parameters, such as pH, initial metal concentrations and contact time. FTIR studies indicate that hydroxyl and carbonyl groups of acids and amides present on the biomass chemically interact with metal ions to ensure complex formation. The kinetic studies of biosorption show greater accordance with the pseudo-second-order model. The biosorption data of Cu(II) fitted well on both the Langmuir and Freundlich adsorption models. It can be understood from these models that single and multiple adsorption layers were built on the *R. fraxinea* biomass for Cu(II) sorption. In the case of Ni(II) sorption, experimental studies show better correlation with the Langmuir isotherm inferring single adsorption layers on the biosorbent. The maximum sorption capacities of Cu(II) and Ni(II) ions by the *R. fraxinea* biomass were calculated from the Langmuir isotherm as 43.48 and 9.71 mg/g, respectively. The calculated thermodynamic parameters show that the nature of the biosorption of Cu(II) and Ni(II) ions onto the *R. fraxinea* biomass was a non-spontaneous endothermic process requiring shaking. This study shows that the biomass of *R. fraxinea* is a moderate biosorbent for the removal of Cu(II) and Ni(II) ions from aqueous solutions compared with other adsorbents.

#### Acknowledgments

The authors wish to thank Dr. Z. Topalcengiz and Mr. E. McQuaid for helpful discussions and manuscript reading. The authors also acknowledge the Anadolu University Research Projects Commission (Project Nos.: 1502F068 and 1605F401) for financial support given.

#### References

- [1] D. Demirezen, A. Aksoy, Accumulation of heavy metals in *Typha angustifolia* (L.) and *Potamogeton pectinatus* (L.) living in Sultan Marsh (Kayseri, Turkey), *Chemosphere*, 56 (2004) 685–696.
- [2] M. Arora, B. Kiran, S. Rani, A. Rani, B. Kaur, N. Mittal, Heavy metal accumulation in vegetables irrigated with water from different sources, *Food Chem.*, 111 (2008) 811–815.
- [3] WHO, Guidelines for Drinking-water Quality, 4th ed., World Health Organization, Geneva, 2011.
- [4] J.O. Duruibe, M.O.C. Ogwuegbu, J.N. Ekwurugwu, Heavy metal pollution and human biotoxic effects, *Int. J. Phys. Sci.*, 2 (2007) 112–118.
- [5] P.B. Tchounwou, C.G. Yedjou, A.K. Patlolla, D.J. Sutton, Heavy metal toxicity and the environment, *Experientia Suppl.*, 101 (2012) 133–164.
- [6] R. Dhankhar, A. Hooda, Fungal biosorption – an alternative to meet the challenges of heavy metal pollution in aqueous solutions, *Environ. Technol.*, 32 (2011) 467–491.
- [7] G.A. Tonini, L.A.M. Ruotolo, Heavy metal removal from simulated wastewater using electrochemical technology: optimization of copper electrodeposition in a membraneless fluidized bed electrode, *Clean Technol. Environ. Policy*, 19 (2017) 403–415.
- [8] F. Fu, Q. Wang, Removal of heavy metal ions from wastewaters: a review, *J. Environ. Manage.*, 92 (2011) 407–418.
- [9] N. Das, R. Vimala, P. Karthika, Biosorption of heavy metals – an overview, *Indian J. Biotechnol.*, 7 (2008) 159–169.
- [10] A. Demirbas, Heavy metal adsorption onto agro-based waste materials: a review, *J. Hazard. Mater.*, 157 (2008) 220–229.
- [11] J.J. Alcaraz-Espinoza, A.E. Chavez-Guajardo, J.C. Medina-Llamas, C.A. Andrade, C.P. de Melo, Hierarchical composite polyaniline-(electrospun polystyrene) fibers applied to heavy metal remediation, *ACS Appl. Mater. Interfaces*, 7 (2015) 7231–7240.



- [12] M. Erdem, S. Ucar, S. Karagoz, T. Tay, Removal of lead (II) ions from aqueous solutions onto activated carbon derived from waste biomass, *Sci. World J.*, 2013 (2013) 1–7.
- [13] N. Sezgin, N. Balkaya, Adsorption of heavy metals from industrial wastewater by using polyacrylic acid hydrogel, *Desal. Wat. Treat.*, 57 (2016) 2466–2480.
- [14] D.H.K. Reddy, S.-M. Lee, Application of magnetic chitosan composites for the removal of toxic metal and dyes from aqueous solutions, *Adv. Colloid Interface Sci.*, 201–202 (2013) 68–93.
- [15] D.H.K. Reddy, Y.-S. Yun, Spinel ferrite magnetic adsorbents: alternative future materials for water purification? *Coord. Chem. Rev.*, 315 (2016) 90–111.
- [16] S. Ucar, M. Erdem, T. Tay, S. Karagoz, Removal of lead(II) and nickel(II) ions from aqueous solution using activated carbon prepared from rapeseed oil cake by  $\text{Na}_2\text{CO}_3$  activation, *Clean Technol. Environ. Policy*, 17 (2015) 747–756.
- [17] M.Y. Cankilic, R.B. Karabacak, T. Tay, M. Kivanc, Sorption of lead ions from aqueous solution onto *Enterococcus faecium* biomass, *Water Sci. Technol.*, 68 (2013) 1550–1555.
- [18] M. Yilmaz, T. Tay, M. Kivanc, H. Turk, Removal of copper(II) ions from aqueous solution by a lactic acid bacterium, *Braz. J. Chem. Eng.*, 27 (2010) 309–314.
- [19] Y. Tunalı, H. Karaca, T. Tay, M. Kivanc, G. Bayramoglu, Biosorption of Pb(II) from aqueous solutions by a fungal biomass in a batch system: equilibrium and kinetic studies, *Asian J. Chem.*, 21 (2009) 6015–6028.
- [20] I. Osasona, O.O. Ajayi, A.O. Adebayo, Equilibrium, kinetics, and thermodynamics of the biosorption of Zn(II) from aqueous solution using powdered cow hooves, *ISRN Phys. Chem.*, 2013 (2013) 1–7.
- [21] L.-e. Liu, J. Liu, H. Li, H. Zhang, J. Liu, H. Zhang, Equilibrium, kinetic, and thermodynamic studies of lead(II) biosorption on sesame leaf, *Bioresources*, 7 (2012) 3555–3572.
- [22] K. Kelly-Vargas, M. Cerro-Lopez, S. Reyna-Tellez, E.R. Bandala, J.L. Sanchez-Salas, Biosorption of heavy metals in polluted water, using different waste fruit cortex, *Phys. Chem. Earth*, 37–39 (2012) 26–29.
- [23] G. Garcia-Rosales, M.T. Olguin, A. Colin-Cruz, E.T. Romero-Guzman, Effect of the pH and temperature on the biosorption of lead(II) and cadmium(II) by sodium-modified stalk sponge of *Zea mays*, *Environ. Sci. Pollut. Res. Int.*, 19 (2012) 177–185.
- [24] G.M. Gadd, Biosorption: critical review of scientific rationale, environmental importance and significance for pollution treatment, *J. Chem. Technol. Biotechnol.*, 84 (2009) 13–28.
- [25] V.B.H. Dang, H.D. Doan, T. Dang-Vu, A. Lohi, Equilibrium and kinetics of biosorption of cadmium(II) and copper(II) ions by wheat straw, *Bioresour. Technol.*, 100 (2009) 211–219.
- [26] M. Calero, F. Hernández, G. Blázquez, M.A. Martín-Lara, G. Tenorio, Biosorption kinetics of Cd(II), Cr(III) and Pb(II) in aqueous solutions by olive stone, *Braz. J. Chem. Eng.*, 26 (2009) 265–273.
- [27] S. Schiewer, S.B. Patil, Modeling the effect of pH on biosorption of heavy metals by citrus peels, *J. Hazard. Mater.*, 157 (2008) 8–17.
- [28] S. Tunalı, A. Cabuk, T. Akar, Removal of lead and copper ions from aqueous solutions by bacterial strain isolated from soil, *Chem. Eng. J.*, 115 (2006) 203–211.
- [29] S. Tunalı, T. Akar, Zn(II) biosorption properties of *Botrytis cinerea* biomass, *J. Hazard. Mater.*, 131 (2006) 137–145.
- [30] R.J. Martins, R. Pardo, R.A. Boaventura, Cadmium(II) and zinc(II) adsorption by the aquatic moss *Fontinalis antipyretica*: effect of temperature, pH and water hardness, *Water Res.*, 38 (2004) 693–699.
- [31] İ. Şahin, S.Y. Keskin, C.S. Keskin, Biosorption of cadmium, manganese, nickel, lead, and zinc ions by *Aspergillus tamarii*, *Desal. Wat. Treat.*, 51 (2013) 4524–4529.
- [32] M. Gavrilescu, Removal of heavy metals from the environment by biosorption, *Eng. Life Sci.*, 4 (2004) 219–232.
- [33] J. Shah, M.R. Jan, A.u. Haq, M. Zeeshan, Equilibrium, kinetic and thermodynamic studies for sorption of Ni (II) from aqueous solution using formaldehyde treated waste tea leaves, *J. Saudi Chem. Soc.*, 19 (2015) 301–310.
- [34] J. Shah, M.R. Jan, S. Jamil, A.u. Haq, Magnetic particles precipitated onto wheat husk for removal of methyl blue from aqueous solution, *Toxicol. Environ. Chem.*, 96 (2014) 218–226.
- [35] J. Shah, M.R. Jan, M. Khan, S. Amir, Removal and recovery of cadmium from aqueous solutions using magnetic nanoparticle-modified sawdust: kinetics and adsorption isotherm studies, *Desal. Wat. Treat.*, 57 (2016) 9736–9744.
- [36] J. Shah, M.R. Jan, A.u. Haq, Removal of lead from aqueous media using carbonized and acid treated orange peel, *Tenside Surfact. Det.*, 51 (2014) 240–246.
- [37] D.H.K. Reddy, D.K.V. Ramana, K. Seshiah, A.V.R. Reddy, Biosorption of Ni(II) from aqueous phase by *Moringa oleifera* bark, a low cost biosorbent, *Desalination*, 268 (2011) 150–157.
- [38] F. Ekmeçyapar, A. Aslan, Y.K. Bayhan, A. Cakici, Biosorption of copper(II) by nonliving lichen biomass of *Cladonia rangiformis* hoffm., *J. Hazard. Mater.*, 137 (2006) 293–298.
- [39] O.D. Uluozlu, A. Sari, M. Tuzen, Biosorption of antimony from aqueous solution by lichen (*Physcia tribacia*) biomass, *Chem. Eng. J.*, 163 (2010) 382–388.
- [40] S. Huneck, I. Yoshimura, Identification of Lichen Substances, Springer, Berlin, New York, 1996.
- [41] D.A. Dias, S. Urban, Chemical constituents of the lichen, *Candelaria concolor*: a complete NMR and chemical degradative investigation, *Nat. Prod. Res.*, 23 (2009) 925–939.
- [42] T.H. Nash, Lichen Biology, Cambridge University Press, Cambridge, New York, 1996.
- [43] T. Tay, M. Candan, M. Erdem, Y. Cimen, H. Turk, Biosorption of cadmium ions from aqueous solution onto non-living lichen *Ramalina fraxinea* biomass, *Clean*, 37 (2009) 249–255.
- [44] K. Turhan, C. Ekinç-Dogan, G. Akcin, A. Asian, Biosorption of Au(III) and Cu(II) from aqueous solution by a non-living *Usnea longissima* biomass, *Fresenius Environ. Bull.*, 14 (2005) 1129–1135.
- [45] M. Hauck, S. Huneck, Lichen substances affect metal adsorption in *Hypogymnia physodes*, *J. Chem. Ecol.*, 33 (2007) 219–223.
- [46] Y. Hannachi, T. Boubaker, Biosorption performance of the lichen biomass (*Diploicia canescens*) for the removal of nickel from aqueous solutions, *Desal. Wat. Treat.*, 57 (2016) 18490–18499.
- [47] A.T. Paulino, J.I. Simonato, J.C. Garcia, J. Nozaki, Characterization of chitosan and chitin produced from silkworm crysalides, *Carbohydr. Polym.*, 64 (2006) 98–103.
- [48] S.P.O. Alvarez, D.A.R. Cadavid, D.M.E. Sierra, C.P.O. Orozco, D.F.R. Vahos, P.Z. Ocampo, L. Atehortua, Comparison of extraction methods of chitin from *Ganoderma lucidum* mushroom obtained in submerged culture, *Biomed. Res. Int.*, 2014 (2014) 1–7.
- [49] P.X. Sheng, Y.-P. Ting, J.P. Chen, L. Hong, Sorption of lead, copper, cadmium, zinc, and nickel by marine algal biomass: characterization of biosorptive capacity and investigation of mechanisms, *J. Colloid Interface Sci.*, 275 (2004) 131–141.
- [50] Y. Liu, Y.-J. Liu, Biosorption isotherms, kinetics and thermodynamics, *Sep. Purif. Technol.*, 61 (2008) 229–242.
- [51] A. Khaled, A. El Nemr, A. El-Sikaily, O. Abdelwahab, Removal of Direct N Blue-106 from artificial textile dye effluent using activated carbon from orange peel: adsorption isotherm and kinetic studies, *J. Hazard. Mater.*, 165 (2009) 100–110.
- [52] K.Y. Foo, B.H. Hameed, Insights into the modeling of adsorption isotherm systems, *Chem. Eng. J.*, 156 (2010) 2–10.
- [53] M. Erdem, E. Yuksel, T. Tay, Y. Cimen, H. Turk, Synthesis of novel methacrylate based adsorbents and their sorptive properties towards *p*-nitrophenol from aqueous solutions, *J. Colloid Interface Sci.*, 333 (2009) 40–48.
- [54] M.E. Argun, S. Dursun, C. Ozdemir, M. Karatas, Heavy metal adsorption by modified oak sawdust: thermodynamics and kinetics, *J. Hazard. Mater.*, 141 (2007) 77–85.
- [55] C. Rozaini, K. Jain, C. Oo, K. Tan, L. Tan, A. Azraa, K. Tong, Optimization of nickel and copper ions removal by modified mangrove barks, *Int. J. Chem. Eng. Appl.*, 1 (2010) 84–89.
- [56] S.R. Shukla, R.S. Pai, Adsorption of Cu(II), Ni(II) and Zn(II) on dye loaded groundnut shells and sawdust, *Sep. Purif. Technol.*, 43 (2005) 1–8.

- [57] D.H.K. Reddy, S.-M. Lee, K. Seshaiiah, Biosorption of toxic heavy metal ions from water environment using honeycomb biomass – an industrial waste material, *Water Air Soil Pollut.*, 223 (2012) 5967–5982.
- [58] H. Yu, J. Pang, T. Ai, L. Liu, Biosorption of  $\text{Cu}^{2+}$ ,  $\text{Co}^{2+}$  and  $\text{Ni}^{2+}$  from aqueous solution by modified corn silk: equilibrium, kinetics, and thermodynamic studies, *J. Taiwan Inst. Chem. Eng.*, 62 (2016) 21–30.
- [59] R.O. Ogbodu, M.O. Omorogie, E.I. Unuabonah, J.O. Babalola, Biosorption of heavy metals from aqueous solutions by *Parkia biglobosa* biomass: equilibrium, kinetics, and thermodynamic studies, *Environ. Prog. Sustain. Energy*, 34 (2015) 1694–1704.
- [60] E. Romera, F. Gonzalez, A. Ballester, M.L. Blazquez, J.A. Munoz, Comparative study of biosorption of heavy metals using different types of algae, *Bioresour. Technol.*, 98 (2007) 3344–3353.
- [61] J. Zhang, K. Yang, H. Wang, B. Lv, F. Ma, Biosorption of copper and nickel ions using *Pseudomonas* sp. in single and binary metal systems, *Desal. Wat. Treat.*, 57 (2016) 2799–2808.
- [62] D.d.Q. Melo, C.B. Vidal, T.C. Medeiros, G.S.C. Raulino, A. Dervanoski, M.d.C. Pinheiro, R.F.d. Nascimento, Biosorption of metal ions using a low cost modified adsorbent (*Mauritia flexuosa*): experimental design and mathematical modeling, *Environ. Technol.*, 37 (2016) 2157–2171.
- [63] S. Karagoz, T. Tay, S. Ucar, M. Erdem, Activated carbons from waste biomass by sulfuric acid activation and their use on methylene blue adsorption, *Bioresour. Technol.*, 99 (2008) 6214–6222.
- [64] P. Maneechakr, S. Karnjanakom, Adsorption behaviour of Fe(II) and Cr(VI) on activated carbon: surface chemistry, isotherm, kinetic and thermodynamic studies, *J. Chem. Thermodyn.*, 106 (2017) 104–112.
- [65] R.M. Ali, H.A. Hamad, M.M. Hussein, G.F. Malash, Potential of using green adsorbent of heavy metal removal from aqueous solutions: adsorption kinetics, isotherm, thermodynamic, mechanism and economic analysis, *Ecol. Eng.*, 91 (2016) 317–332.